



HAL
open science

FINITE VOLUME METHOD FOR THE CAHN-HILLIARD EQUATION WITH DYNAMIC BOUNDARY CONDITIONS

Flore Nabet

► **To cite this version:**

Flore Nabet. FINITE VOLUME METHOD FOR THE CAHN-HILLIARD EQUATION WITH DYNAMIC BOUNDARY CONDITIONS. 2013. hal-00872690v2

HAL Id: hal-00872690

<https://hal.science/hal-00872690v2>

Preprint submitted on 24 Jan 2014 (v2), last revised 18 May 2014 (v3)

HAL is a multi-disciplinary open access archive for the deposit and dissemination of scientific research documents, whether they are published or not. The documents may come from teaching and research institutions in France or abroad, or from public or private research centers.

L'archive ouverte pluridisciplinaire **HAL**, est destinée au dépôt et à la diffusion de documents scientifiques de niveau recherche, publiés ou non, émanant des établissements d'enseignement et de recherche français ou étrangers, des laboratoires publics ou privés.

FINITE VOLUME METHOD FOR THE CAHN-HILLIARD EQUATION WITH DYNAMIC BOUNDARY CONDITIONS

FLORE NABET¹

Abstract. In this paper, we investigate a numerical scheme for solving a diphasic Cahn-Hilliard model with dynamic boundary conditions. We propose a finite volume method for the space discretization and we prove existence and convergence results. We also present numerical simulations to show the influence of these boundary conditions.

1. INTRODUCTION

The Cahn-Hilliard equation describes the evolution of binary mixtures which appears, for example, when a binary alloy is cooled down sufficiently. This problem has been extensively studied for many years with Neumann boundary conditions. Recently, physicists [4, 5, 7] have introduced new boundary conditions, usually called dynamic boundary conditions, to account for the effective interaction between the wall and the two mixture components for a confined system. With these dynamic boundary conditions, the Cahn-Hilliard system is written as follows: Find the concentration $c : [0, T] \times \Omega \rightarrow \mathbb{R}$ such that:

$$\left\{ \begin{array}{ll} \partial_t c = \Gamma_b \Delta \mu, & \text{in } (0, T) \times \Omega; \\ \mu = -\varepsilon \sigma_b \Delta c + \frac{\sigma_b}{\varepsilon} f'_b(c), & \text{in } (0, T) \times \Omega; \\ c(0, \cdot) = c_0, & \text{in } \Omega; \\ \frac{\varepsilon^3}{\Gamma_s \Gamma_b} \partial_t c_\Gamma = \varepsilon^2 \sigma_s \sigma_b \Delta_{\parallel} c_\Gamma - \sigma_b f'_s(c_\Gamma) - \varepsilon \sigma_b \partial_n c, & \text{on } (0, T) \times \Gamma; \\ \partial_n \mu = 0, & \text{on } (0, T) \times \Gamma; \end{array} \right. \quad (\mathcal{P})$$

where μ is an intermediate unknown called chemical potential. There cannot be any mass exchange through the boundary, that is why we have Neumann boundary condition for the chemical potential. The domain $\Omega \subset \mathbb{R}^2$ is smooth connected and bounded, we denote by $\Gamma = \partial\Omega$ its boundary and $T > 0$ is the final time.

We denote by Δ_{\parallel} the Laplace-Beltrami operator on Γ , ∂_n the exterior normal derivative at the boundary and c_Γ the trace of c on Γ .

The parameter $\varepsilon > 0$ accounts for the interface thickness, the coefficient $\Gamma_b > 0$ is the bulk mobility and $\sigma_b > 0$ is the fluid-fluid surface tension. On the boundary, $\Gamma_s > 0$ defines a surface kinetic coefficient and $\sigma_s > 0$ a surface capillarity coefficient. The nonlinear terms f'_b and f'_s represent the bulk free energy density and the surface free energy density respectively and they satisfy the following assumptions:

¹ Aix-Marseille Université, CNRS, Centrale Marseille, LATP, UMR 7353, 13453, Marseille, France (flore.nabet@univ-amu.fr).

- Dissipativity:

$$\liminf_{|x| \rightarrow \infty} f_b''(x) > 0 \quad \text{and} \quad \liminf_{|x| \rightarrow \infty} f_s''(x) > 0. \quad (\mathcal{H}_{diss})$$

- Polynomial growth for f_b : there exists $C_b > 0$ and a real $p \geq 2$ such that:

$$\begin{aligned} |f_b(x)| &\leq C_b (1 + |x|^p), \\ |f_b'(x)| &\leq C_b (1 + |x|^{p-1}), \\ |f_b''(x)| &\leq C_b (1 + |x|^{p-2}). \end{aligned} \quad (\mathcal{H}_{f_b})$$

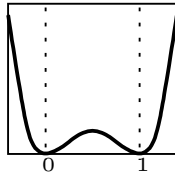


FIGURE 1. Typical choice for f_b : $f_b(c) = c^2(1-c)^2$.

Remark 1.1. We can notice that if we choose $\sigma_s = 0$, $\Gamma_s = +\infty$ and $f_s = 0$, we recover the standard Neumann boundary condition $\partial_n c = 0$.

The Cahn-Hilliard equation with dynamic boundary conditions (\mathcal{P}) is posed in order that the following free energy functional,

$$\mathcal{F}(c) = \int_{\Omega} \left(\frac{\varepsilon}{2} \sigma_b |\nabla c|^2 + \frac{\sigma_b}{\varepsilon} f_b(c) \right) + \int_{\Gamma} \left(\frac{\varepsilon^2}{2} \sigma_s \sigma_b |\nabla_{\parallel} c_{\Gamma}|^2 + \sigma_b f_s(c_{\Gamma}) \right), \quad (1)$$

will decrease with respect to time:

$$\frac{d}{dt} \mathcal{F}(c(t, \cdot)) = -\Gamma_b \int_{\Omega} |\nabla \mu(t, \cdot)|^2 - \frac{\varepsilon^3}{\Gamma_s \Gamma_b} \int_{\Gamma} |\partial_t c_{\Gamma}(t, \cdot)|^2, \quad t \in [0, T].$$

From a mathematical point of view, the problem (\mathcal{P}) has already been studied in [8–10] where questions such as global existence and uniqueness, existence of global attractor, maximal regularity of solutions and convergence to an equilibrium have been answered. From a numerical point of view, some numerical schemes have been considered in [4, 5, 7] in a finite difference framework but without proof of convergence. In [2], the authors propose a finite element space semi-discretization and prove error estimate and convergence results on a slab with periodic conditions on the lateral directions and dynamic conditions on the vertical directions, so that complex geometries of the domain are not taken into account in the convergence analysis.

In this paper, we investigate a finite volume scheme for the space discretization of this problem. This discretization is well adapted to the curved geometry and to the coupling between the dynamics in the domain and the one on the boundary by a flux term. In Section 2, we recall the main finite volume notations, for example used in [3], that we adapt to our problem with curved domain and dynamic boundary conditions. In Section 3, we give the discrete energy functional and the associated energy estimates. Then, we propose a finite volume scheme with different time discretizations for the nonlinear terms. Existence and convergence results are stated in Section 4. The convergence result enables in particular to get a proof of the existence of a weak solution of the Cahn-Hilliard model with dynamic boundary conditions. Finally, we give some numerical results in Section 5 with different nonlinear terms on the boundary.

2. THE DISCRETE FRAMEWORK

We give in this section the main notations and definitions used in this paper.

2.1. The discretization

We notice that Ω is a curved domain so that the notations (Fig. 2) and definitions are slightly different than the usual finite volume definitions given for example in [3].

An admissible mesh \mathcal{T} is constituted by an interior mesh \mathfrak{M} and a boundary mesh $\partial\mathfrak{M}$. The interior mesh \mathfrak{M} is a set of control volumes (we notice that some control volumes are curved) $\mathcal{K} \subset \Omega$ such that:

- if $\kappa \neq \mathcal{L}$, we have $\hat{\kappa} \cap \hat{\mathcal{L}} = \emptyset$;
- if $\kappa \neq \mathcal{L}$ such that the dimension of $\bar{\kappa} \cap \bar{\mathcal{L}}$ is equal to 1, then $\bar{\kappa} \cap \bar{\mathcal{L}}$ is an edge of the mesh;
- $\cup_{\mathcal{K} \in \mathfrak{M}} \bar{\mathcal{K}} = \bar{\Omega}$.

We denote by $\partial\mathfrak{M}$ the set of edges σ (we remark that these are not segments but curve sections) of the control volumes in \mathfrak{M} included in Γ . Let \mathcal{E} be the set of the edges of the mesh \mathcal{T} , $\mathcal{E}_{int} = \mathcal{E} \setminus \partial\mathfrak{M}$ the set of interior edges and \mathcal{V} the set of the vertices included in Γ .

For each control volume $\mathcal{K} \in \mathfrak{M}$, we associate a point $x_{\mathcal{K}} \in \kappa$ and we assume that for all neighbouring control volumes $\kappa, \mathcal{L} \in \mathfrak{M}$ the edge $\sigma = \kappa|\mathcal{L}$ is orthogonal to the straight line going through x_{κ} and $x_{\mathcal{L}}$. The distance between x_{κ} and $x_{\mathcal{L}}$ is denoted by $d_{\kappa, \mathcal{L}}$ and m_{σ} is the length of σ . Let m_{κ} be the Lebesgue measure of κ and if κ is a curved control volume then m_{κ}^{app} is the area of the polygon formed by the vertices of κ . We denote by \mathcal{E}_{κ} the set of its edges and $\bar{\mathbf{n}}_{\sigma\kappa}$ the outward unit normal vector to κ .

For any $\sigma \in \partial\mathfrak{M}$, we denote by e_{σ} the chord associated with σ , $m_{e_{\sigma}}$ its length and $\bar{\mathbf{n}}_{e_{\sigma}}$ the outward unit normal vector to Ω . Let x_{σ} on Γ as defined on the Figure 2 and such that e_{σ} is orthogonal to the straight line going through x_{κ} and x_{σ} , then y_{σ} is the intersection between the line (x_{κ}, x_{σ}) and the chord e_{σ} . We denote by $d_{\kappa, \sigma}$ the distance between x_{κ} and y_{σ} , \mathcal{V}_{σ} the set of vertices of σ and $\bar{\mathbf{n}}_{\sigma}$ the outward unit normal vector to Ω .

Let $\mathbf{v} = \sigma|\sigma'$ be the vertex which separates the edges $\sigma, \sigma' \in \partial\mathfrak{M}$, $\gamma_{\mathbf{v}} \subset \Gamma$ the arch whose ends are x_{σ} and $x_{\sigma'}$ and $m_{\gamma_{\mathbf{v}}}$ its length. We denote by $d_{\sigma, \mathbf{v}}$ the distance between y_{σ} and \mathbf{v} and $d_{\sigma, \sigma'}$ is equal to the sum of $d_{\sigma, \mathbf{v}}$ and $d_{\sigma', \mathbf{v}}$.

We can notice that we do not use the equation of the curve. Indeed, we only know the coordinates of the vertices of the mesh and so these quantities are calculated from these coordinates.

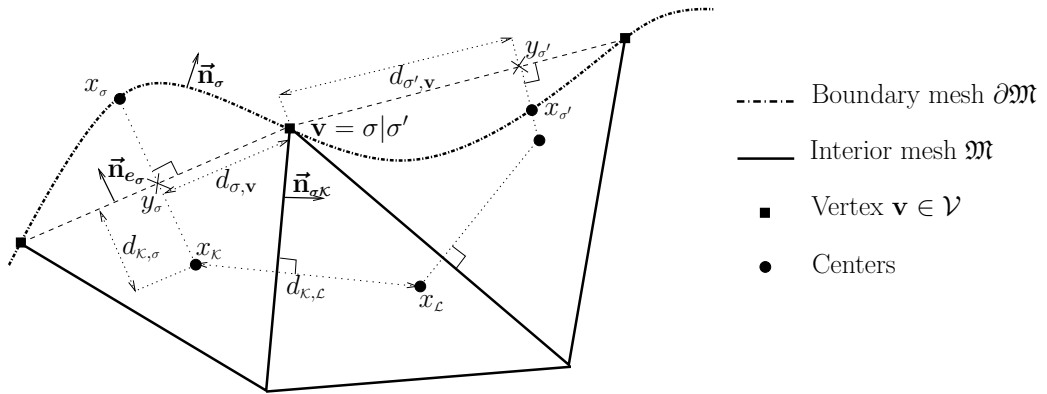


FIGURE 2. Finite volume meshes

The mesh size is defined by: $\text{size}(\mathcal{T}) = \sup\{\text{diam}(\kappa), \kappa \in \mathfrak{M}\}$. All the constants in the results below depend on a certain measure of the regularity of the mesh which is classical and that we do not make explicit here in order to be more synthetic. In short, it is necessary that the control volumes do not become flat when the mesh is refined.

Let $N \in \mathbb{N}^*$ and $T \in]0, +\infty[$. The temporal interval $[0, T]$ is uniformly discretized with a fixed time step $\Delta t = \frac{T}{N}$. For $n \in \{0, \dots, N\}$, we define $t^n = n\Delta t$.

2.2. Discrete unknowns

For a given time step t^n , the FV method associates with all interior control volumes $\mathcal{K} \in \mathfrak{M}$ an unknown value $c_{\mathcal{K}}^n \in \mathbb{R}^{\mathfrak{M}}$ and with all exterior edges $\sigma \in \partial\mathfrak{M}$ an unknown value $c_{\sigma}^n \in \mathbb{R}^{\partial\mathfrak{M}}$ for the order parameter. The same notations are used for the chemical potential with an unknown value $\mu_{\mathcal{K}}^n \in \mathbb{R}^{\mathfrak{M}}$ for all $\mathcal{K} \in \mathfrak{M}$. There is no need of boundary unknowns for μ .

Whenever it is convenient, we associate with a discrete function $u_{\mathcal{T}} \in \mathbb{R}^{\mathcal{T}}$ the piecewise constant functions $u_{\mathcal{T}} = (u_{\mathfrak{M}}, u_{\partial\mathfrak{M}})$ where $u_{\mathfrak{M}} = \sum_{\mathcal{K} \in \mathfrak{M}} u_{\mathcal{K}} 1_{\mathcal{K}} \in L^{\infty}(\Omega)$ and $u_{\partial\mathfrak{M}} = \sum_{\sigma \in \partial\mathfrak{M}} u_{\sigma} 1_{\sigma} \in L^{\infty}(\Gamma)$.

We denote by $u_{\mathcal{T}}^{\Delta t}$ the piecewise constant function in $]0, T[\times \Omega$ such that for all $t \in [t^n, t^{n+1}[$:

$$u_{\mathcal{T}}^{\Delta t}(t, x) = u_{\mathcal{K}}^{n+1} \text{ if } x \in \mathcal{K} \quad \text{and} \quad u_{\mathcal{T}}^{\Delta t}(t, x) = u_{\sigma}^{n+1} \text{ if } x \in \sigma.$$

2.3. Discrete inner products and norms

Definition 2.1 (Discrete L^2 norms).

- For $u_{\mathfrak{M}} \in \mathbb{R}^{\mathfrak{M}}$, the L^2 discrete norm of $u_{\mathfrak{M}}$ is defined by:

$$\|u_{\mathfrak{M}}\|_{0, \mathfrak{M}}^2 = \sum_{\mathcal{K} \in \mathfrak{M}} m_{\mathcal{K}} u_{\mathcal{K}}^2.$$

- For $u_{\partial\mathfrak{M}} \in \mathbb{R}^{\partial\mathfrak{M}}$, the L^2 discrete norm of $u_{\partial\mathfrak{M}}$ is defined by:

$$\|u_{\partial\mathfrak{M}}\|_{0, \partial\mathfrak{M}}^2 = \sum_{\sigma \in \partial\mathfrak{M}} m_{e_{\sigma}} u_{\sigma}^2.$$

Definition 2.2 (Discrete H^1 semi-definite inner products).

- For $u_{\mathcal{T}}, v_{\mathcal{T}} \in \mathbb{R}^{\mathcal{T}}$, their H^1 discrete semi-definite inner product is defined by:

$$\llbracket u_{\mathcal{T}}, v_{\mathcal{T}} \rrbracket_{1, \mathcal{T}} = \sum_{\sigma \in \mathcal{E}_{int}} m_{\sigma} d_{\mathcal{K}, \mathcal{L}} \left(\frac{u_{\mathcal{K}} - u_{\mathcal{L}}}{d_{\mathcal{K}, \mathcal{L}}} \right) \left(\frac{v_{\mathcal{K}} - v_{\mathcal{L}}}{d_{\mathcal{K}, \mathcal{L}}} \right) + \sum_{\sigma \in \partial\mathfrak{M}} m_{e_{\sigma}} d_{\mathcal{K}, \sigma} \left(\frac{u_{\mathcal{K}} - u_{\sigma}}{d_{\mathcal{K}, \sigma}} \right) \left(\frac{v_{\mathcal{K}} - v_{\sigma}}{d_{\mathcal{K}, \sigma}} \right),$$

where, by convention, $u_{\sigma} = u_{\mathcal{K}}$ for $\sigma \in \partial\mathfrak{M}$ an edge of \mathcal{K} if $u_{\mathcal{T}}$ satisfies homogeneous Neumann boundary condition. We notice by $|u_{\mathcal{T}}|_{1, \mathcal{T}} = \llbracket u_{\mathcal{T}}, u_{\mathcal{T}} \rrbracket_{1, \mathcal{T}}^{\frac{1}{2}}$ the associated discrete H^1 seminorm in Ω .

- For $u_{\partial\mathfrak{M}}, v_{\partial\mathfrak{M}} \in \mathbb{R}^{\partial\mathfrak{M}}$, their H^1 discrete semi-definite inner product is defined by:

$$\llbracket u_{\partial\mathfrak{M}}, v_{\partial\mathfrak{M}} \rrbracket_{1, \partial\mathfrak{M}} = \sum_{\nu \in \mathcal{V}} d_{\sigma, \sigma'} \left(\frac{u_{\sigma} - u_{\sigma'}}{d_{\sigma, \sigma'}} \right) \left(\frac{v_{\sigma} - v_{\sigma'}}{d_{\sigma, \sigma'}} \right).$$

We notice by $|u_{\partial\mathfrak{M}}|_{1, \partial\mathfrak{M}} = \llbracket u_{\partial\mathfrak{M}}, u_{\partial\mathfrak{M}} \rrbracket_{1, \partial\mathfrak{M}}^{\frac{1}{2}}$ the associated discrete H^1 seminorm on Γ .

Now, we can define H^1 discrete norms by:

$$\|u_{\mathcal{T}}\|_{1, \mathcal{T}}^2 = \|u_{\mathcal{T}}\|_{0, \mathfrak{M}}^2 + |u_{\mathcal{T}}|_{1, \mathcal{T}}^2, \quad \forall u_{\mathcal{T}} \in \mathbb{R}^{\mathcal{T}} \quad \text{and} \quad \|u_{\partial\mathfrak{M}}\|_{1, \partial\mathfrak{M}}^2 = \|u_{\partial\mathfrak{M}}\|_{0, \partial\mathfrak{M}}^2 + |u_{\partial\mathfrak{M}}|_{1, \partial\mathfrak{M}}^2, \quad \forall u_{\partial\mathfrak{M}} \in \mathbb{R}^{\partial\mathfrak{M}}.$$

3. NUMERICAL SCHEME AND ENERGY ESTIMATES

3.1. Numerical scheme

We use a consistent two point flux approximation for Laplace operators in Ω and a consistent two point flux approximation for the Laplace-Beltrami operator on Γ . For nonlinear terms, we use two different discretizations described below: fully implicit and semi implicit so that we have to use a Newton method at each iteration.

We assume that $c_{\mathcal{T}}^n \in \mathbb{R}^{\mathcal{T}}$ is given, the scheme is then written as follows.

Problem 3.1. Find $(c_{\mathcal{T}}^{n+1}, \mu_{\mathfrak{M}}^{n+1}) \in \mathbb{R}^{\mathcal{T}} \times \mathbb{R}^{\mathfrak{M}}$ such that $\forall \gamma_{\mathcal{T}} \in \mathbb{R}^{\mathcal{T}}, \forall \nu_{\mathfrak{M}} \in \mathbb{R}^{\mathfrak{M}}$, we have:

$$\left\{ \begin{array}{l} \sum_{\kappa \in \mathfrak{M}} m_{\kappa}^{app} \frac{c_{\kappa}^{n+1} - c_{\kappa}^n}{\Delta t} \nu_{\kappa} = -\Gamma_b \llbracket \mu_{\mathfrak{M}}^{n+1}, \nu_{\mathfrak{M}} \rrbracket_{1, \mathcal{T}} \\ \sum_{\kappa \in \mathfrak{M}} m_{\kappa}^{app} \mu_{\kappa}^{n+1} \gamma_{\kappa} = \frac{\sigma_b}{\varepsilon} \sum_{\kappa \in \mathfrak{M}} m_{\kappa}^{app} df^b(c_{\kappa}^n, c_{\kappa}^{n+1}) \gamma_{\kappa} \\ \quad + \varepsilon \sigma_b \left(\sum_{\sigma \in \mathcal{E}_{int}} m_{\sigma} d_{\kappa, \mathcal{L}} \left(\frac{c_{\kappa}^{n+1} - c_{\mathcal{L}}^{n+1}}{d_{\kappa, \mathcal{L}}} \right) \left(\frac{\gamma_{\kappa} - \gamma_{\mathcal{L}}}{d_{\kappa, \mathcal{L}}} \right) + \boxed{\sum_{\sigma \in \partial \mathfrak{M}} m_{e_{\sigma}} \left(\frac{c_{\kappa}^{n+1} - c_{\sigma}^{n+1}}{d_{\kappa, \sigma}} \right) \gamma_{\kappa}} \right) \\ \frac{\varepsilon^3}{\Gamma_b \Gamma_s} \sum_{\sigma \in \partial \mathfrak{M}} m_{e_{\sigma}} \frac{c_{\sigma}^{n+1} - c_{\sigma}^n}{\Delta t} = -\varepsilon^2 \sigma_b \sigma_s \llbracket c_{\partial \mathfrak{M}}^{n+1}, \gamma_{\partial \mathfrak{M}} \rrbracket_{1, \partial \mathfrak{M}} - \sigma_b \sum_{\sigma \in \partial \mathfrak{M}} m_{e_{\sigma}} df^s(c_{\sigma}^n, c_{\sigma}^{n+1}) \gamma_{\sigma} \\ \quad - \varepsilon \sigma_b \boxed{\sum_{\sigma \in \partial \mathfrak{M}} m_{e_{\sigma}} \left(\frac{c_{\sigma}^{n+1} - c_{\kappa}^{n+1}}{d_{\kappa, \sigma}} \right) \gamma_{\sigma}} \end{array} \right. \quad (\mathcal{S})$$

The functions df^b and df^s represent the discretizations for nonlinear terms.

We can notice that in the scheme (\mathcal{S}) the coupling between interior and boundary unknowns is performed by the two boxed terms: one in the interior mesh \mathfrak{M} and the other on the boundary mesh $\partial \mathfrak{M}$.

In order to simplify the presentation and the analysis, we have written the scheme as a formulation which looks like a variational formulation. However, if for each control volume we choose the indicator function of this particular control volume as a test function in (\mathcal{S}) , we recognize a usual finite volume flux balance equation.

3.2. Energy estimate

In the section we give the definition of the discrete energy and the corresponding estimate.

Definition 3.2 (Discrete free energy). The discrete free energy associated with the continuous free energy (1) is composed of a bulk energy $\mathcal{F}_{\mathfrak{M}}^b$ and a surface energy $\mathcal{F}_{\partial \mathfrak{M}}^s$ such that for all $c_{\mathcal{T}} \in \mathbb{R}^{\mathcal{T}}$:

$$\mathcal{F}_{\mathcal{T}}(c_{\mathcal{T}}) = \mathcal{F}_{\mathfrak{M}}^b(c_{\mathcal{T}}) + \mathcal{F}_{\partial \mathfrak{M}}^s(c_{\partial \mathfrak{M}})$$

where:

$$\mathcal{F}_{\mathfrak{M}}^b(c_{\mathcal{T}}) = \frac{\sigma_b}{\varepsilon} \sum_{\kappa \in \mathfrak{M}} m_{\kappa}^{app} f_b(c_{\kappa}) + \frac{\varepsilon}{2} \sigma_b |c_{\mathcal{T}}|_{1, \mathcal{T}}^2 \quad \text{and} \quad \mathcal{F}_{\partial \mathfrak{M}}^s(c_{\partial \mathfrak{M}}) = \sigma_b \sum_{\sigma \in \partial \mathfrak{M}} m_{e_{\sigma}} f_s(c_{\sigma}) + \frac{\varepsilon^2}{2} \sigma_b \sigma_s |c_{\partial \mathfrak{M}}|_{1, \partial \mathfrak{M}}^2.$$

By using Problem 3.1 with $\nu_{\mathfrak{M}} = \mu_{\mathfrak{M}}^{n+1}$ and $\gamma_{\mathcal{T}} = c_{\mathcal{T}}^{n+1} - c_{\mathcal{T}}^n$ as test functions, we obtain the following energy estimate.

Proposition 3.3 (General energy estimate). *Let $c_{\mathcal{T}}^n \in \mathbb{R}^{\mathcal{T}}$. We assume that there exists a solution $(c_{\mathcal{T}}^{n+1}, \mu_{\mathfrak{M}}^{n+1})$ of Problem 3.1. Then, the following equality holds:*

$$\begin{aligned} & \mathcal{F}_{\mathcal{T}}(c_{\mathcal{T}}^{n+1}) - \mathcal{F}_{\mathcal{T}}(c_{\mathcal{T}}^n) + \Delta t \Gamma_b |\mu_{\mathfrak{M}}^{n+1}|_{1, \mathcal{T}}^2 + \frac{\varepsilon^3}{\Gamma_b \Gamma_s} \frac{1}{\Delta t} \|c_{\partial \mathfrak{M}}^{n+1} - c_{\partial \mathfrak{M}}^n\|_{0, \partial \mathfrak{M}}^2 \\ & + \frac{\varepsilon}{2} \sigma_b |c_{\mathcal{T}}^{n+1} - c_{\mathcal{T}}^n|_{1, \mathcal{T}}^2 + \frac{\varepsilon^2}{2} \sigma_b \sigma_s |c_{\partial \mathfrak{M}}^{n+1} - c_{\partial \mathfrak{M}}^n|_{1, \partial \mathfrak{M}}^2 \\ & = \frac{\sigma_b}{\varepsilon} \sum_{\kappa \in \mathfrak{M}} m_{\kappa}^{app} (f_b(c_{\kappa}^{n+1}) - f_b(c_{\kappa}^n) - df^b(c_{\kappa}^n, c_{\kappa}^{n+1})(c_{\kappa}^{n+1} - c_{\kappa}^n)) \\ & + \sigma_b \sum_{\sigma \in \partial \mathfrak{M}} m_{e_{\sigma}} (f_s(c_{\sigma}^{n+1}) - f_s(c_{\sigma}^n) - df^s(c_{\sigma}^n, c_{\sigma}^{n+1})(c_{\sigma}^{n+1} - c_{\sigma}^n)). \end{aligned} \quad (2)$$

3.3. Discretization for nonlinear terms

In this section, we detail the two discretizations for nonlinear terms used in the scheme (\mathcal{S}) and we give the associated energy estimates.

3.3.1. Fully implicit discretization

For the fully implicit discretization in time, we choose d^{f_b} and d^{f_s} independent of $c_{\mathcal{K}}^n$, for all $\mathcal{K} \in \mathfrak{M}$ and for all $\sigma \in \partial\mathfrak{M}$, we have:

$$d^{f_b}(c_{\mathcal{K}}^n, c_{\mathcal{K}}^{n+1}) = f'_b(c_{\mathcal{K}}^{n+1}) \quad \text{and} \quad d^{f_s}(c_{\sigma}^n, c_{\sigma}^{n+1}) = f'_s(c_{\sigma}^{n+1}).$$

Then, by using the energy estimate (2) and dissipativity assumptions (\mathcal{H}_{diss}) , we obtain the following discrete energy inequality:

Proposition 3.4 (Discrete energy inequality). *Let $c_{\mathcal{T}}^n \in \mathbb{R}^{\mathcal{T}}$. We assume that there exists a solution $(c_{\mathcal{T}}^{n+1}, \mu_{\mathfrak{M}}^{n+1})$ of Problem 3.1. Then, there exists $\Delta t_0 > 0$ such that for all $\Delta t \leq \Delta t_0$, we have:*

$$\begin{aligned} \mathcal{F}_{\mathcal{T}}(c_{\mathcal{T}}^{n+1}) + \frac{\Delta t \Gamma_b}{2} |\mu_{\mathfrak{M}}^{n+1}|_{1,\mathcal{T}}^2 + \frac{\varepsilon^3}{\Gamma_b \Gamma_s} \frac{1}{2\Delta t} \|c_{\partial\mathfrak{M}}^{n+1} - c_{\partial\mathfrak{M}}^n\|_{0,\partial\mathfrak{M}}^2 \\ + \frac{\varepsilon}{4} \sigma_b |c_{\mathcal{T}}^{n+1} - c_{\mathcal{T}}^n|_{1,\mathcal{T}}^2 + \frac{\varepsilon^2}{2} \sigma_b \sigma_s |c_{\partial\mathfrak{M}}^{n+1} - c_{\partial\mathfrak{M}}^n|_{1,\partial\mathfrak{M}}^2 \leq \mathcal{F}_{\mathcal{T}}(c_{\mathcal{T}}^n). \end{aligned}$$

We can notice that Δt_0 depends on parameters of the equation so with this discretization, we have to choose Δt small enough. This is why we introduce below another discretization.

3.3.2. Semi implicit discretization

We would like to obtain an energy estimate without condition on Δt . Thus, we choose a discretization for nonlinear terms such that the right terms in (2) are equal to 0:

$$d^{f_b}(x, y) = \frac{f_b(y) - f_b(x)}{y - x} \quad \text{and} \quad d^{f_s}(x, y) = \frac{f_s(y) - f_s(x)}{y - x}, \quad \forall x, y.$$

We obtain the following energy equality available for all $\Delta t > 0$:

Proposition 3.5 (Discrete energy equality). *Let $c_{\mathcal{T}}^n \in \mathbb{R}^{\mathcal{T}}$. We assume that there exists a solution $(c_{\mathcal{T}}^{n+1}, \mu_{\mathfrak{M}}^{n+1})$ of Problem 3.1, then we have:*

$$\begin{aligned} \mathcal{F}_{\mathcal{T}}(c_{\mathcal{T}}^{n+1}) + \Delta t \Gamma_b |\mu_{\mathfrak{M}}^{n+1}|_{1,\mathcal{T}}^2 + \frac{\varepsilon^3}{\Gamma_b \Gamma_s} \frac{1}{\Delta t} \|c_{\partial\mathfrak{M}}^{n+1} - c_{\partial\mathfrak{M}}^n\|_{0,\partial\mathfrak{M}}^2 \\ + \frac{\varepsilon}{2} \sigma_b |c_{\mathcal{T}}^{n+1} - c_{\mathcal{T}}^n|_{1,\mathcal{T}}^2 + \frac{\varepsilon^2}{2} \sigma_b \sigma_s |c_{\partial\mathfrak{M}}^{n+1} - c_{\partial\mathfrak{M}}^n|_{1,\partial\mathfrak{M}}^2 = \mathcal{F}_{\mathcal{T}}(c_{\mathcal{T}}^n). \end{aligned}$$

4. EXISTENCE AND CONVERGENCE

We give general assumptions on the discretization of nonlinear potential d^{f_b} to demonstrate existence and convergence theorems.

d^{f_b} is of \mathcal{C}^1 class and there exist $C_b \geq 0$ and a real p such that $2 \leq p < +\infty$,

$$\begin{aligned} |d^{f_b}(a, b)| &\leq C_b (1 + |a|^{p-1} + |b|^{p-1}) \\ |D(d^{f_b}(a, \cdot))(b)| &\leq C_b (1 + |a|^{p-2} + |b|^{p-2}). \end{aligned} \tag{\mathcal{H}_{d^{f_b}}}$$

4.1. Existence

The existence of a solution to discrete Problem 3.1 is based on the topological degree theory and the a priori energy estimates obtained above.

Theorem 4.1 (Existence of discrete solution). *Let $c_\tau^n \in \mathbb{R}^\tau$. Assume that dissipativity assumptions (\mathcal{H}_{diss}) and growth conditions (\mathcal{H}_{df_b}) hold and that there exist constants $K_b^{c_\tau^n}, K_s^{c_\tau^n}$ (depending possibly on c_τ^n) such that, for all $\gamma_\tau \in \mathbb{R}^\tau$,*

$$\begin{aligned} \sum_{\kappa \in \mathfrak{M}} m_\kappa^{app} (f_b(\gamma_\kappa) - f_b(c_\kappa^n) - df_b(c_\kappa^n, \gamma_\kappa)(\gamma_\kappa - c_\kappa^n)) &\leq K_b^{c_\tau^n}, \\ \sum_{\sigma \in \partial \mathfrak{M}} m_{e_\sigma} (f_s(\gamma_\sigma) - f_s(c_\sigma^n) - df_s(c_\sigma^n, \gamma_\sigma)(\gamma_\sigma - c_\sigma^n)) &\leq K_s^{c_\tau^n}. \end{aligned} \quad (3)$$

Then, there exists at least one solution $(c_\tau^{n+1}, \mu_\tau^{n+1}) \in \mathbb{R}^\tau \times \mathbb{R}^{\mathfrak{M}}$ of Problem 3.1.

4.2. Convergence

In order to prove the convergence result we have to define a solution of Problem (\mathcal{P}) in a weak sense.

Definition 4.2 (Weak formulation). We say that a couple $(c, \mu) \in L^\infty(0, T; H^1(\Omega)) \times L^2(0, T; H^1(\Omega))$ such that $\text{Tr}(c) \in L^\infty(0, T; H^1(\Gamma))$ is solution to the continuous Problem (\mathcal{P}) in the weak sense if for all $\psi \in C_c^\infty([0, T] \times \overline{\Omega})$, the following identities hold:

$$\int_0^T \int_\Omega (-\partial_t \psi c + \Gamma_b \nabla \mu \cdot \nabla \psi) = \int_\Omega c^0 \psi(0, \cdot), \quad (4)$$

$$\begin{aligned} \int_0^T \int_\Omega \left(-\mu \psi + \varepsilon \sigma_b \nabla c \cdot \nabla \psi + \frac{\sigma_b}{\varepsilon} f'_b(c) \psi \right) + \int_0^T \int_\Gamma \left(-\frac{\varepsilon^3}{\Gamma_b \Gamma_s} \partial_t \psi c + \sigma_s \sigma_b \varepsilon^2 \nabla_\parallel c \cdot \nabla_\parallel \psi + \sigma_b f'_s(c) \psi \right) \\ = \frac{\varepsilon^3}{\Gamma_b \Gamma_s} \int_\Gamma c^0 \psi(0, \cdot). \end{aligned} \quad (5)$$

Theorem 4.3 (Bounds of solutions). *Assume that assumptions (\mathcal{H}_{f_b}), (\mathcal{H}_{diss}), (\mathcal{H}_{df_b}), (3) hold and that there exists a constant $C > 0$ such that, for all $n \in \mathbb{N}$,*

$$\begin{aligned} \mathcal{F}_\tau(c_\tau^{n+1}) + C \left(\Delta t \Gamma_b \|\mu_\tau^{n+1}\|_{1, \tau}^2 + \frac{\varepsilon^3}{\Gamma_b \Gamma_s} \frac{1}{\Delta t} \|c_\tau^{n+1} - c_\tau^n\|_{0, \partial \mathfrak{M}}^2 + \frac{\varepsilon}{2} \sigma_b \|c_\tau^{n+1} - c_\tau^n\|_{1, \tau}^2 + \frac{\varepsilon^2}{2} \sigma_b \sigma_s \|c_\tau^{n+1} - c_\tau^n\|_{1, \partial \mathfrak{M}}^2 \right) \\ \leq \mathcal{F}_\tau(c_\tau^n). \end{aligned} \quad (6)$$

Then, there exists $M > 0$ independent of \mathcal{T} and Δt such that:

$$\begin{aligned} \sup_{n \leq N} \|c_\tau^n\|_{1, \tau} \leq M, \quad \sup_{n \leq N} \|c_\tau^n\|_{1, \partial \mathfrak{M}} \leq M, \quad \sum_{n=0}^{N-1} \Delta t \|\mu_\tau^{n+1}\|_{1, \tau}^2 \leq M, \\ \Delta t \sum_{n=0}^{N-1} \Delta t \left\| \frac{c_\tau^{n+1} - c_\tau^n}{\Delta t} \right\|_{1, \tau}^2 \leq M \quad \text{and} \quad \Delta t \sum_{n=0}^{N-1} \Delta t \left\| \frac{c_\tau^{n+1} - c_\tau^n}{\Delta t} \right\|_{1, \partial \mathfrak{M}}^2 \leq M. \end{aligned}$$

These bounds are one of the key elements to prove the convergence result below by using discrete H^1 compactness and Kolmogorov theorem. We also notice that we have nonlinearities in the domain Ω and on the boundary Γ . Thus $L^2((0, T) \times \Omega)$ compactness is not sufficient and we have to prove uniform estimates of time and space translates on Ω and Γ .

Theorem 4.4 (Estimation of time and space translates). *Let $(c_{\tau}^{\Delta t}, \mu_{\partial\mathfrak{M}}^{\Delta t})$ be a solution of Problem 3.1, then there exists $C > 0$ (not depending on $\text{size}(\mathcal{T})$ and Δt) such that:*

$$\begin{aligned} \left\| \widetilde{c_{\partial\mathfrak{M}}^{\Delta t}}(\cdot + \tau, \cdot) - \widetilde{c_{\partial\mathfrak{M}}^{\Delta t}}(\cdot, \cdot) \right\|_{L^2(\mathbb{R} \times \mathbb{R}^2)}^2 &\leq C\tau, & \left\| \widetilde{c_{\partial\mathfrak{M}}^{\Delta t}}(\cdot, \cdot + \eta) - \widetilde{c_{\partial\mathfrak{M}}^{\Delta t}}(\cdot, \cdot) \right\|_{L^2(\mathbb{R} \times \mathbb{R}^2)}^2 &\leq C|\eta|(|\eta| + \text{size}(\mathcal{T})), \\ \left\| \widetilde{c_{\partial\mathfrak{M}}^{\Delta t}}(\cdot + \tau, \cdot) - \widetilde{c_{\partial\mathfrak{M}}^{\Delta t}}(\cdot, \cdot) \right\|_{L^2(\mathbb{R} \times \Gamma)}^2 &\leq C\tau, & \left\| \widetilde{c_{\partial\mathfrak{M}}^{\Delta t}}(\cdot, \tau_{\eta}(\cdot)) - \widetilde{c_{\partial\mathfrak{M}}^{\Delta t}}(\cdot, \cdot) \right\|_{L^2(\mathbb{R} \times \Gamma)}^2 &\leq C|\eta|(|\eta| + \text{size}(\mathcal{T})), \end{aligned}$$

where we denote by $\widetilde{c_{\partial\mathfrak{M}}^{\Delta t}}$ (respectively $\widetilde{c_{\partial\mathfrak{M}}^{\Delta t}}$) the extension by 0 of $c_{\partial\mathfrak{M}}^{\Delta t}$ (respectively $c_{\partial\mathfrak{M}}^{\Delta t}$) on $\mathbb{R} \times \mathbb{R}^2$ (respectively $\mathbb{R} \times \Gamma$) and τ_{η} represent the shifting of length η along the boundary Γ (an orientation being given on Γ).

The Theorem 4.4 is proved by using bounds of solutions of Theorem 4.3 and the scheme (S). This Theorem is essential to apply Kolmogorov theorem and to prove the following convergence result.

Theorem 4.5 (Convergence theorem). *Assume that conditions (\mathcal{H}_{f_b}) , (\mathcal{H}_{diss}) , (\mathcal{H}_{df_b}) , (3) and (6) hold. Consider the Problem (P) with initial condition $c_0 \in H^1(\Omega)$ such that $\text{Tr}(c_0) \in H^1(\Gamma)$. Then, there exists a weak solution (c, μ) on $[0, T]$ (in the sense of Definition 4.2). Furthermore, let $(c^{(m)}, c_{\Gamma}^{(m)})_{m \in \mathbb{N}}$ and $(\mu^{(m)})_{m \in \mathbb{N}}$ be a sequence of solutions to Problem 3.1 with a sequence of discretizations such that the space and time step, $\text{size}(\mathcal{T}^{(m)})$ and $\Delta t^{(m)}$ respectively, tends to 0. Then, up to a subsequence, the following convergence properties hold, for all $q \geq 1$, when $\text{size}(\mathcal{T}^{(m)})$, $\Delta t^{(m)} \rightarrow 0$:*

$$\begin{aligned} c^{(m)} &\rightarrow c \text{ in } L^2(0, T; L^q(\Omega)) \text{ strong,} \\ c_{\Gamma}^{(m)} &\rightarrow \text{Tr}(c) \text{ in } L^2(0, T; L^q(\Gamma)) \text{ strong,} \\ \text{and } \mu^{(m)} &\rightarrow \mu \text{ in } L^2(0, T; L^q(\Omega)) \text{ weak.} \end{aligned}$$

Remark 4.6. We choose the initial concentration in the scheme equals to the mean-value projection:

$$c_{\tau}^0 = \left(\left(\frac{1}{m_{\kappa}} \int_{\mathcal{K}} c_0 \right)_{\kappa \in \mathfrak{M}}, \left(\frac{1}{m_{\sigma}} \int_{\sigma} c_0 \right)_{\sigma \in \partial\mathfrak{M}} \right).$$

5. NUMERICAL SIMULATIONS

In this section, we present numerical experiments for three different choices of the nonlinear surface free energy density. We choose here the semi-implicit discretization in time for nonlinear terms in order to take Δt large enough. We notice that we have to choose the interface thickness ε of the same order (and not more large) than the mesh size $\text{size}(\mathcal{T})$. For each simulation we consider the usual double well bulk potential $f_b(c) = c^2(1 - c)^2$.

We are interested here by two domains with a delaunay triangular mesh:

- a rectangle $(0, 8) \times (0, 4)$ with periodic boundary conditions in the lateral direction and dynamic boundary conditions in the vertical direction;
- a smooth curved domain whose diameter is equal to 2 and dynamic boundary conditions everywhere on Γ .

In these cases, x_{κ} is the circumcenter of the control volume κ and y_{σ} is the middle of the chord e_{σ} .

For each domain, we choose a random initial $c^0 \in \mathbb{R}^{\mathcal{T}}$ between 0.4 and 0.6 and we keep this initial data for each simulation with the same domain. We can then observe the influence of the boundary conditions on the phase separation dynamics.

5.1. Influence of the surface diffusion term

First, we choose $f_s = f_b$ for the surface potential and to compare the results in [4, 5], we begin with the rectangular domain (Fig. 3) and the following parameters: $\varepsilon = 0.3$, $\Gamma_b = \sigma_b = 0.1$ for the bulk, $\Gamma_s = 10$ for the

surface and $T = 0.75$, $dt = 0.05$ for the time. We observe the influence of surface diffusion by computing the scheme with two different values for the surface coefficient σ_s .

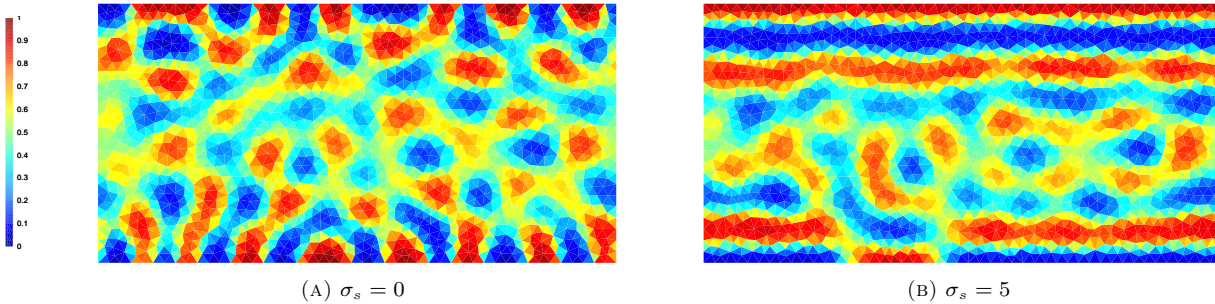


FIGURE 3. Spinodal decomposition for rectangular domain

In both case, we have lateral anisotropic structures but their length scale is different. Indeed, when we have $\sigma_s = 0$ (Fig. 3a) the structure length scales are shorter than when we have $\sigma_s = 5$ (Fig. 3b). These results are very close to those observed in [4].

Now, we test the scheme with our curved domain (Fig. 4) with following parameters: $\varepsilon = \Gamma_b = \sigma_b = 0.1$ for the bulk, $\Gamma_s = 10$ for the surface and $T = 0.025$, $dt = 0.005$ for the time.

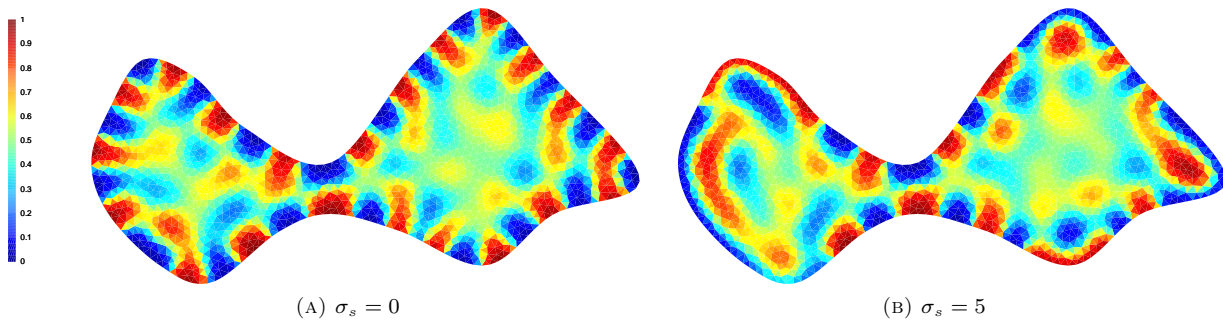


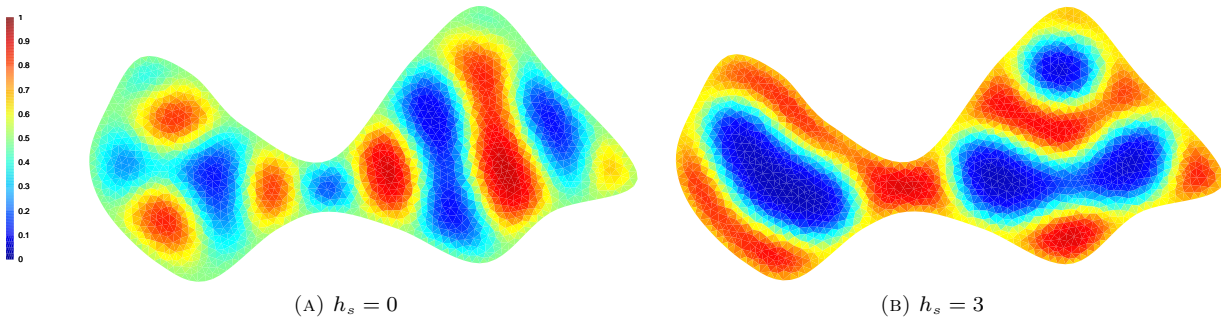
FIGURE 4. Spinodal decomposition for curved domain

We observe the same behavior as for the rectangular domain (Fig. 3): for $\sigma_s = 0$ (Fig. 4a), we have small typical structures on the boundary while for $\sigma_s = 5$ (Fig. 4a) the structures are large except where the domain is too narrow.

5.2. Preferential attraction by the wall

For the following computation (Fig 5), we want to observe the influence of the surface potential by taking $f_s(c) = g_s c^2 - (h_s + g_s)c$ where $h_s \neq 0$ describes the possible preferential attraction of one of the two components by the wall. Thus, we choose fixed parameters: $\varepsilon = 0.2$, $\Gamma_b = \sigma_b = 0.1$ for the bulk, $\Gamma_s = 10$, $\sigma_s = 0$, $g_s = 10$ for the surface and $T = 0.37$, $dt = 0.001$ for the time and we modify the coefficient h_s .

First, we notice than the parallel structures observed when $h_s = 0$ (Fig. 5a) are similar to those observed in [2, 7]. Then, we confirm the preferential attraction of the phase $c = 1$ by the boundary when $h_s > 0$ (Fig. 5b) and we notice that this attraction changes all the behavior in the domain Ω .

FIGURE 5. Influence of h_s

CONCLUSION

We propose here a finite volume scheme to deal with the 2D Cahn-Hilliard model with dynamic boundary conditions. With this method the coupling between the equation in the domain and the equation on the boundary is easy to implement with a curved geometry for the mesh. Furthermore, the convergence result enables to obtain the existence of weak solutions for the continuous problem. We can notice that some authors are interested by the Cahn-Hilliard equation with logarithmic potential (see for example [1,6] and the references therein) but it is not the case in this work.

REFERENCES

- [1] Laurence Cherfilis, Alain Miranville, and Sergey Zelik. The Cahn-Hilliard equation with logarithmic potentials. *Milan J. Math.*, 79(2):561–596, 2011.
- [2] Laurence Cherfilis, Madalina Petcu, and Morgan Pierre. A numerical analysis of the Cahn-Hilliard equation with dynamic boundary conditions. *Discrete Contin. Dyn. Syst.*, 27(4):1511–1533, 2010.
- [3] Robert Eymard, Thierry Gallouët, and Raphaële Herbin. *Finite volume methods*. Handb. Numer. Anal., VII. North-Holland, Amsterdam, 2000.
- [4] Hans Peter Fischer, Philipp Maass, and Wolfgang Dieterich. Novel surface modes in spinodal decomposition. *Phys. Rev. Lett.*, 79:893–896, Aug 1997.
- [5] Hans Peter Fischer, Philipp Maass, and Wolfgang Dieterich. Diverging time and length scales of spinodal decomposition modes in thin films. *EPL (Europhysics Letters)*, 42(1):49–54, 1998.
- [6] Gianni Gilardi, Alain Miranville, and Giulio Schimperna. Long time behavior of the Cahn-Hilliard equation with irregular potentials and dynamic boundary conditions. *Chin. Ann. Math. Ser. B*, 31(5):679–712, 2010.
- [7] R. Kenzler, F. Eurich, P. Maass, B. Rinn, J. Schropp, E. Bohl, and W. Dieterich. Phase separation in confined geometries: Solving the Cahn-Hilliard equation with generic boundary conditions. *j-COMP-PHYS-COMM*, 133:139–157, Jan 2001.
- [8] Jan Prüss, Reinhard Racke, and Songmu Zheng. Maximal regularity and asymptotic behavior of solutions for the Cahn-Hilliard equation with dynamic boundary conditions. *Ann. Mat. Pura Appl. (4)*, 185(4):627–648, 2006.
- [9] Reinhard Racke and Songmu Zheng. The Cahn-Hilliard equation with dynamic boundary conditions. *Adv. Differential Equations*, 8(1):83–110, 2003.
- [10] Hao Wu and Songmu Zheng. Convergence to equilibrium for the Cahn-Hilliard equation with dynamic boundary conditions. *J. Differential Equations*, 204(2):511–531, 2004.